2016 IEEE International Conference on Robotics and Automation (ICRA)
Stockholm, Sweden, May 16-21, 2016

Robot-Human Balance State Transfer during Full-Body Humanoid Teleoperation Using Divergent Component of Motion Dynamics

Joao Ramos[1], Albert Wang[1] and Sangbae Kim[1]

Abstract— **This paper presents the ongoing work towards enabling humanoid robots to achieve dynamic behaviors comparable to humans. By using the concept of Divergent Component of Motion (DCM) first in introduced in [1], the present paper permits operator and robot balance synchronization using the mutual dynamics of the Center of Mass (CoM) and Center of Pressure (CoP). The Linear Inverted Pendulum Model (LIPM) with a reaction mass [2] is utilized to capture the humanoid behavior which interacts with the human operator under the Equilibrium Point (EP) [3] control assumption. Remarkable similarities between the physical system behavior and simulated results suggest the feasibility of the strategy. Experiments conducted with the MIT HERMES humanoid robot further show the performance of the proposed method.**

I. Introduction

Humans are inherently talented when adapting to novel situations and possess highly creative problem-solving skills that state-of-the-art robotic platforms still cannot achieve. This ability motivated us to explore human intelligence and motor skills to reliably deploy robots to dangerous or unpredictable environments, such as disaster scenarios. In addition, human motor control generates elegant and smooth simultaneous coordination of several joints, taking advantage of one's own body dynamics in order to carry out complex dynamic tasks, such as building momentum to push heavy objects or to swing a bat. A clear question is thus how to take advantage of human natural control capabilities and use it to coordinate multi-joint machines. One intuitive solution is to directly capture and imitate human actions through whole-body teleoperation. And, to enhance this experience, give the operator all the stimuli necessary for complete immersion in the robot's body. By allowing the operator to feel the external forces and disturbances experienced by the robot, one can use their own innate reflex-based motor skills in order to guide the robot to perform complex dynamic tasks.

Our previous work using a novel Balance Feedback Interface (BFI) [4] and [5] showed that we can utilize the robot Center of Pressure (CoP) and support polygon information in order to achieve semi-static balance. The BFI is a six DOF device that applies external forces to the operator's waist in proportion to the degree of instability of the robot. Following these results, this paper introduces the use of the robot Divergent Component of Motion (DCM) [6] as a mean to allow the operator to command dynamic robot CoM motions and to obtain feedback about the humanoid state of balance. The use of the DCM has allowed researchers in [7] and [8] to achieve dynamic legged locomotion. Hence we expect that the DCM can be explored to achieve high momentum-delivery tasks such as swinging a heavy object.

Fig. 1. MIT HERMES humanoid robot designed for highly dynamic power manipulation tasks.

On the Linear Inverted Pendulum Model (LIPM) the DCM (or Capture Point [1], or Extrapolated Center of Mass [9]) represents the first order equilibrium point of the CoM dynamics, suggesting that it may play a key role for bilateral dynamic teleoperation. In [8] this idea is extended in order to generate an online dynamic walking pattern for a biped robot by manipulating the virtual repellent point. The work in [7] and [10] use the DCM of a model with variable natural frequency in order to regulate the robot linear and angular momentum for stable standing and walking under external disturbances. Furthermore, the work by [11] is inspired on the optimal regulator in order to design a CoM/CoP controller inspired by the DCM. These authors explore the concept of the stabilization of the equilibrium state of the CoM in order to improve disturbance robustness. We propose the use of DCM as a way to inform the human operator about the robot state of balance.

Many authors make use of teleoperation for multi-joint coordination of robotic platform with many DOF. In the case of humanoid robots, control strategies range from the use of Motion Capture Suits (MoCap) for online [12] and offline

[1]Authors are with the Department of Mechanical Engineering, Massachusetts Institute of Technology, Cambridge MA, USA
*Corresponding author jlramos@mit.edu

[13] trajectory generation, to the use of hand manipulated scale marionettes [14] or joysticks [15]. But in all these cases, the operation is either unilateral (no feedback to human) or the feedback does not explore human reflex-based motor control skills. Similar to our work, [16] and [17] explore the idea of feeding back to the human the forces applied to the robot through an inverted pendulum model mapping, allowing the human to teach the robot how to comply to external forces and while stabilizing inside the support region. The paper also focus on machine learning and autonomy but not on direct whole-body imitation. Hence, the author's strategy does not extend to the complexity or bandwidth of the movements required for power manipulation applications. In [18], the authors utilize a camera-based human MoCap strategy to extract motion commands and generate dynamically stable movements; but the operator is unaware about the robot state.

With the strategy presented in this work, we expect to use human proprioceptive feedback (inherently faster than visual [19]) to allow the robot to take advantage of human creative full-body solutions to maintain balance while carrying out complex dynamic tasks.

This paper is organized as follows. Section II presents the legged robot model and the identification of the appropriate linear model for the human CoM dynamics. Section III presents the overall system interactions and simulation results. Section IV shows experiments conducted with the real human-size robot and section V addresses some conclusions and give a brief overview of the future work.

II. System Modelling and Hypothesis

A. Robot Model

MIT HERMES is a robotic platform designed to achieve power manipulation which requires explosive limb motions. As the robot is designed with very lightweight limbs (around 3kg each) the torso accounts for about 75% of the total mass (45kg). Thus, we use the Inverted Pendulum with a reaction mass (see Fig. 2) model to simulate the robot CoM dynamics. Future work expect to incorporate linear and angular momentum control on the stabilization strategy using the body inertia [20]. The massless prismatic legs of variable length d connect the actuated ankle joint to the CoM of mass m_R; the torso with inertia I_R is controlled by the torque τ_2. An external force F_{ext} is assumed to be applied to the CoM at position $x_R = \begin{bmatrix} x_{COM} & z_{COM} \end{bmatrix}^T$. States p_x and ξ_x represents the robot CoP and DCM, respectively.

The linear equations of motion for the model are given by

$$\begin{bmatrix} m_R {d_0}^2 & 0 & I_R \\ 0 & m_R & 0 \\ I_R & 0 & I_R \end{bmatrix} \ddot{q} + \begin{bmatrix} -m_R g d_0 \theta_1 \\ m_R g \\ 0 \end{bmatrix} = \begin{bmatrix} \tau_1 \\ F_l \\ \tau_2 \end{bmatrix} + \begin{bmatrix} d_0 F_{ext} \\ 0 \\ 0 \end{bmatrix}, \tag{1}$$

where d_0 represents a constant leg length, g is the gravity magnitude and the state vector is given by $q = \begin{bmatrix} \theta_1 & d & \theta_2 \end{bmatrix}^T$.

The DCM for the LIPM is defined as the equilibrium convergence point of the robot CoM as $t \to \infty$ [11] and is

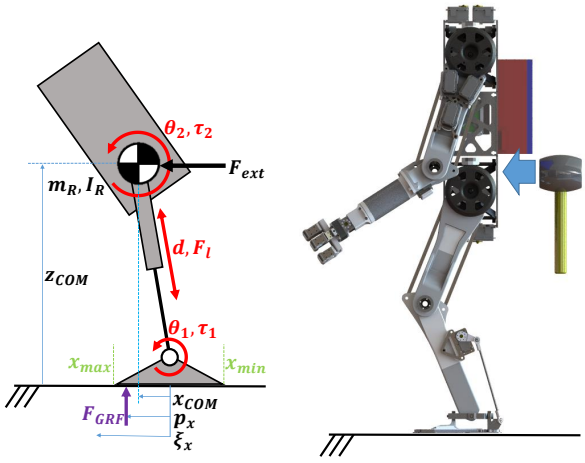

Fig. 2. Left: robot model: Linear Inverted Prismatic Pendulum with reaction mass. Right: MIT HERMES is hit by hammer near the robot CoM to generate external disturbance.

defined as

$$\xi_x = x_{COM} + \frac{\dot{x}_{COM}}{\omega}. \tag{2}$$

On which $\omega = \sqrt{\frac{g + \ddot{z}_{COM}}{z_{COM}}}$ is the pendulum natural frequency. Assuming $\ddot{z}_{COM} = 0$ and taking the time derivative of (2) we have

$$\dot{\xi}_x = \dot{x}_{COM} + \frac{\ddot{x}_{COM}}{\omega}, \tag{3}$$

$$\dot{\xi}_x = \omega \xi_x - \omega x_{COM} + \frac{F_{ext}}{m_R \omega}. \tag{4}$$

Equation (4) utilizes the fact that $F_{ext} = m_R \ddot{x}_{COM}$ and shows the direct dependency of the DCM dynamics with the externally applied forces. Also, by solving (2) for $\dot{x}_{COM}$ we can see that ξ_x represents the first order stable dynamics for the CoM, or

$$\dot{x}_{COM} = -\omega (x_{COM} - \xi_x). \tag{5}$$

This results implies that the robot CoM can be stabilized by controlling the DCM state. Thus, as the robot tracks human CoM position, the DCM error can be mapped to force applied to the operator CoM and inform about the robot stability.

When inside the support polygon, the CoP for the inverted pendulum with a reaction mass is given by the point on the ground where the reaction force statically balances the ankle torque [2]. In other words

$$p_x = -\frac{\tau_1}{m_R g}. \tag{6}$$

B. Human Model

The human body is a very complex system to be precisely modeled. We assume significant simplifications in order to capture particular behaviors during specific tasks. The work in [3] explores a promising model of Equilibrium Point (EP) control. In this model, human central nervous

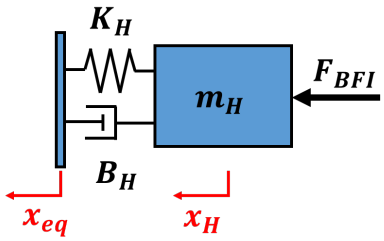

Fig. 3. Human CoM model: Equilibrium Point control assumption.

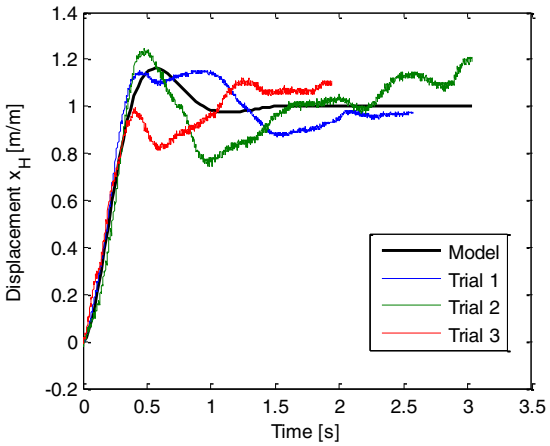

Fig. 4. Normalized human CoM 2^{nd} dynamic response to step forces F_{BFI} applied by the Balance Feedback Interface.

system generates an equilibrium state for the body posture and controls the muscles impedance around that equilibrium point.In the current work we assume the operator performs EP control for the CoM state, see Fig. 3. The Balance Feedback Interface produces an external force F_{BFI} near the operator CoM (with total mass m_H), which regulates a linear stiffness K_H and damper B_H around the equilibrium state x_{eq}.

To evaluate the fidelity of the model, three experimental trials were conducted in which forces were applied to the subject waist with different magnitudes and on both directions perpendicular the frontal plane. Fig. 4 shows the normalized displacement due to different step forces when the equilibrium state is assumed to be zero ($x_{eq} = 0$); it also shows the second order model adopted as

$$\frac{X_H}{F_{BFI}} = \frac{1}{K_H} \frac{\omega_n^2}{s^2 + 2\zeta\omega_n s + \omega_n^2}. \tag{7}$$

On (7) X_H is the Laplace transform of displacement variable x_H. Moreover, K_H, ζ, and ω_n represent human CoM DC gain, damping ratio and natural frequency, respectively. These constants were estimated by fitting a second order model as verified on Fig. 4.

III. Closed-Loop System and Simulations

The MIT HERMES teleoperation system is comprehended of two core subsystems: (i) the Master, which is composed of the MoCap suit, BFI and operator; and (ii) the Slave, the HERMES robot. As shown on [5] the system enables full-body teleoperation with bilateral feedback. The slave platform generates joint impedance around the equilibrium states that are mapped from the operator motion. As the robot is disturbed by the environment the BFI generates forces that are applied to the human waist accordingly. The system architecture can be seen on Fig. 5.

The gain α is the scaling factor between robot and human world coordinates; the robot tracks CoM and CoP position $\begin{bmatrix} x_{ref} & \dot{x}_{ref} & p_{xref} \end{bmatrix}^T$ from the human reference. The vector $\begin{bmatrix} \delta\xi_x & \delta p_{xref} \end{bmatrix}^T$ is the tracking error that is utilized by the BFI to generate the feedback force. Finally, C_{robot} represents the robot joint controller that takes into account the inverse CoM kinematics and generates joint torques τ_R.

In [21] the author proposes an optimal CoM/CoP controller to achieve maximum standing region. The work in [11] shows an equivalent controller that assumes CoP first order dynamics and DCM feedback. For this paper we utilize the following feedback law:

$$K_{BFI} = -\begin{bmatrix} k_\xi & k_{px} \end{bmatrix} \tag{8}$$

Thus,

$$F_{BFI} = -k_\xi \delta\xi_x - k_{px}\delta p_x. \tag{9}$$

As the CoP can be used as a metric of standing stability we also use this state on the feedback law: if the CoP remains inside the support polygon the robot can prevent falling.

Notice that the sign on the BFI gain (8) is negative. Thus, if the robot is, for example, pushed forward the human will receive a feedback force to move backwards. In this situation, the human act as a low pass filter and the control structure take advantage of human passive dynamics (before neural feedback) for the first portion (around 50ms) of the response [4], allowing for a faster reaction. If the sign was positive, the operator would be disturbed on the same direction of the robot. In this scenario, on the other hand, human neural feedback loop would act as the active robot controller to regain stability. As a conclusion, we hypothesize that for large external forces that require fast reactions the negative feedback should be more appropriate; but for smaller F_{ext} that can be mitigated with slower reaction, positive feedback could be more appropriated to improve the systems performance. For the current work, only negative feedback is explored.

We can derive two equations from the block diagram on Fig. 5:

$$X_R = \alpha X_H \frac{C_R H_R}{1 + C_R H_R} + F_{ext} \frac{H_R}{1 + C_R H_R}, \tag{10}$$

$$X_H = X_{eq} \frac{C_H H_H}{1 + C_H H_H} + F_{BFI} \frac{H_H}{1 + C_H H_H}. \tag{11}$$

One can see the similarity on both systems dynamics. On (10) and (11) C_i, and H_i represent the subsystem controller and plant transfer function, respectively ($i = [R, H]$). The dependency on the dynamics between both system is defined by the gains α and K_{BFI}, increasing one gain or another increases mutual stability dependency.

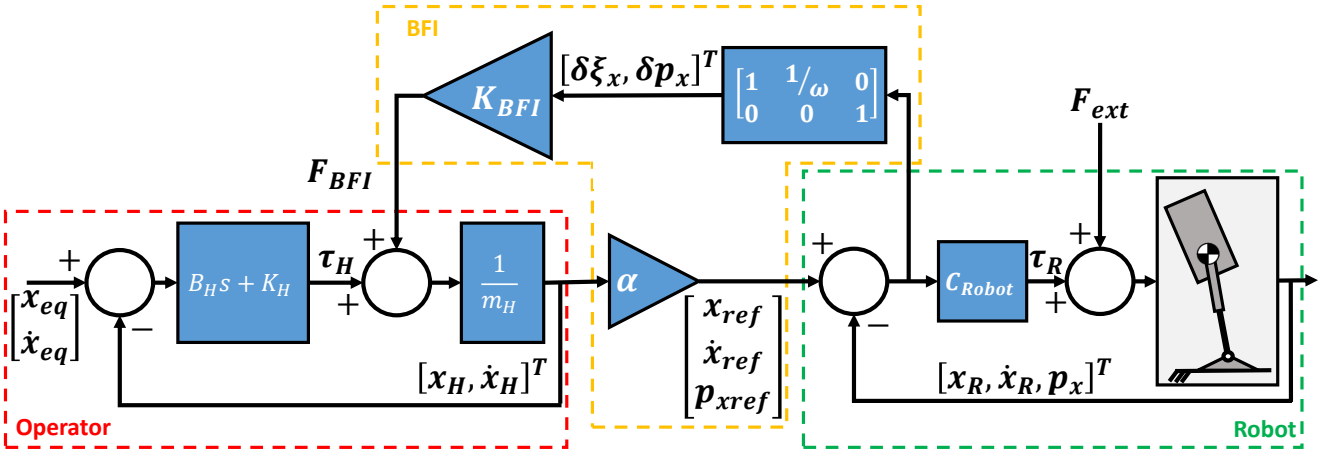

Fig. 5. Block Diagram for the MIT HERMES system with bilateral feedback on the sagittal plane. Both the operator and robot are closed-loop systems, and the BFI is represented by the transmission that couples these two systems .

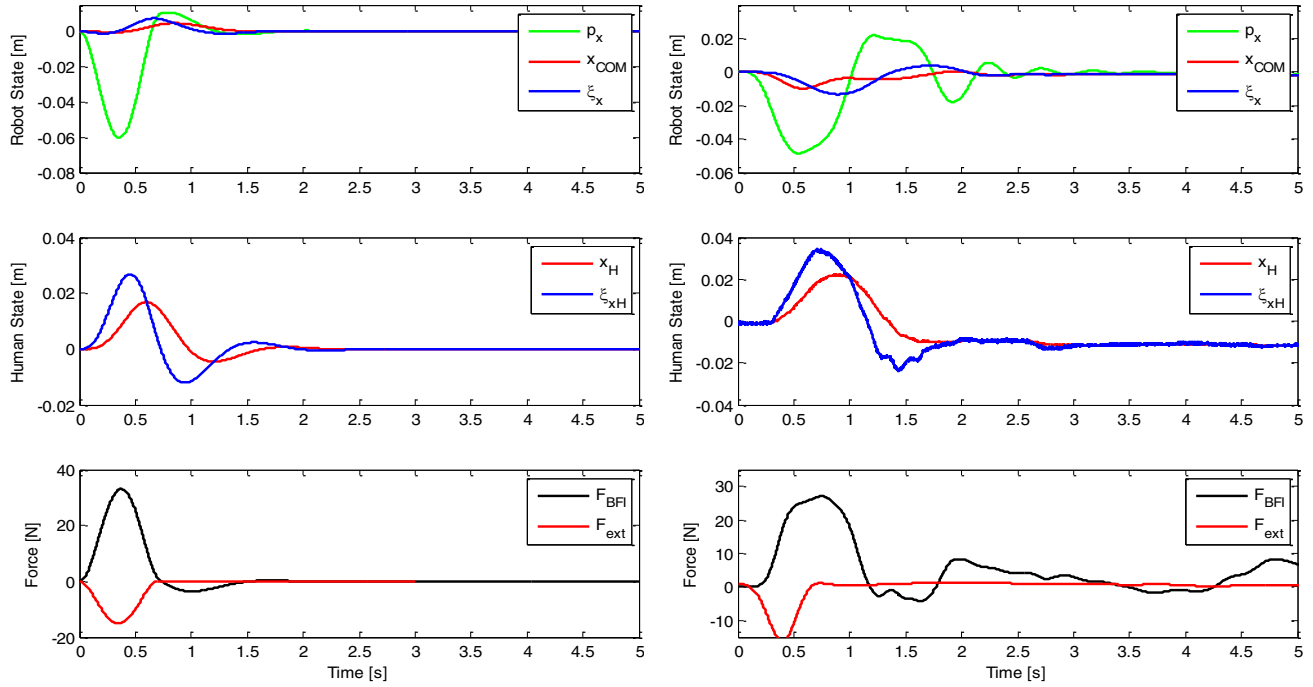

Fig. 6. Top Left: Predicted robot dynamics under impact. Top right: Measured robot dynamics under impact disturbance. Mid Left: Predicted human dynamics. Mid Right: Measured human dynamics. Bottom Left: Estimated external force applied to the robot and BFI force applied to human. Bottom Right: Measured external force applied to the robot and BFI force applied to human.

Fig. 6 shows the simulation of the human and robot interaction when the robot is subject to an external force with 15N peak magnitude. The robot support polygon limit is at $\begin{bmatrix}x_{min} & x_{max}\end{bmatrix} = \begin{bmatrix}-60 & 115\end{bmatrix} mm$.

IV. Experimental Results

An experiment with the physical system was conducted to evaluate the proposed control strategy and the results were compared to the model hypothesis. During the experiment the human operator is asked to comfortably stand inside the BFI wearing the MoCap suit, being able to move freely within a small area with both feet stationary on the ground. Although the user possessed control authority over the upper limbs, it was asked that they should not be used for disturbance rejection (e.g. swinging arms for momentum regulation). The teleoperated humanoid stood on a flat and smooth surface with arms down and struck at the front mid-torso by an instrumented hammer (F_{ext}). Parameters of the controller are

TABLE I

SYSTEM EXPERIMENTAL PARAMETERS.

System Parameter	Value
Gain k_ξ on ξ_x	600 N/m
Gain k_{px} on p_x	500 N/m
Mapping Gain $\alpha = \frac{\theta_2^{ref}}{x_H}$	2 rad/m

given in Table I. The robot CoP is measured by six load cells under the robot feet (three per foot) [4].

The force profile from the hammer was measured from the experiment and approximated to be applied to the model. The comparison of model and experiment is shown in Fig. 6. The three plots on the left are the predicted results while the three right plots show the measured data from the physical system: robot and human states. A side-by-side comparison shows that the features of the data collected from the simulated model closely match the key behaviors from the experiment. Therefore, it is safe to assume that the model is a competent description of the system behavior within the linear assumed range and with the current coupling strategy between the robot and human operator.

The timing and phasing of the force applied to the robot (F_{ext}) and to the human (F_{BFI}) show corresponding trends; following similar magnitudes as the simulated counterparts. However, the time profile for the physical system is longer (slower dynamics) and we can identify slight phase delay caused by force generation bandwidth. The additional ripples after 1.5s are likely caused by motor detent torque or cogging in the actuators that generate forces on the human operator.

As shown on (9) the force generated by the BFI is dependent on the robot Center of Pressure (p_x) and DCM (ξ_x). This can be observed by the coinciding peaks of p_x and the force at operator on the top and bottom graphs respectively. Due to light damping in the observed human dynamics, it was necessary to add a damping term on the force for reducing ringing (these oscillations can still be observed on the top right plot of Fig. 6). The states x_R and ξ_x display a single value and peak that appear in shorter duration for the simulated system. We assume that the overall system delay is caused primarily by unmodeled communication delay and actuator bandwidth (approximately 45ms time constant). Human state dynamics present a remarkable similarity to the proposed equilibrium point model. Small discrepancies could be caused by muscle stiffness variation due to neural activation feedback and other small nonlinearities.

Finally, the overall system display slower dynamics, with longer duration oscillatory periods. Nonetheless the remarkably linear system behavior is closely captured by the simulated experiment. The proposed model has sufficient fidelity despite disregarded additional dynamics and state estimation approximations (human and robot CoM). Fig. 7 shows an extended experiment over 30 seconds in which the robot is struck five time with different intensities (at approximately 1s, 10s, 15s, 18s, and 22s). The measured force on the human operator F_{BFI} is simulated with equation

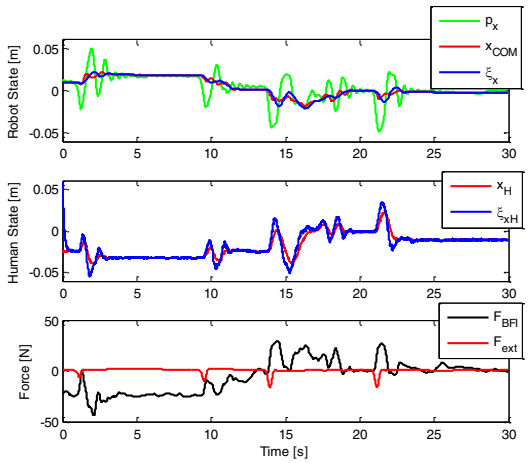

Fig. 7. Thirty second experimental balancing task in which the robot receives several external forces near the robot CoM generated by an instrumented hammer.

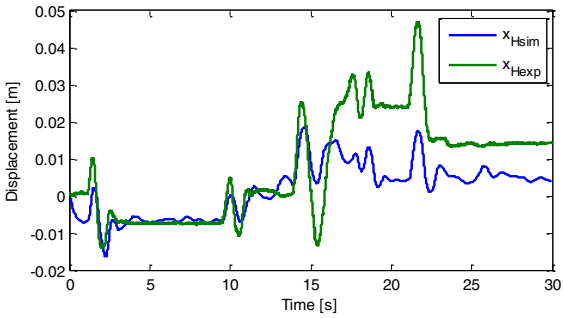

Fig. 8. Comparison of the predicted human CoM displacement x_{Hsim} with the same state measured from the BFI displacement x_{Hexp}.

(7) to obtain a simulated human CoM position x_{Hsim}. The simulated operator position is compared to actual position x_{Hexp} in Fig. 8. Notice that the discrepancies between the steady state value is likely due to the variation of human equilibrium state x_{eq} which is the internal unknown neural command to the human muscles.

Additional insights on how to design controllers to synchronize the robot and operator can be obtained from the proposed model. A gain value of $\alpha = 2rad/m$ was chosen for the hardware experiment so the CoM would move approximately the same amount in both the robot and human. Fig. 9 shows the simulation result from a gain value of $\alpha = 3rad/m$ and demonstrates the sensitivity to the mapping gain. The system is destabilized by an initial external disturbance force profile of magnitude -15N over 0.5s.

V. CONCLUSION AND FUTURE WORK

In this work, a simple model for the bilateral feedback teleoperation dynamics is proposed and its fidelity is evaluated using the MIT HERMES humanoid robot under similar disturbances. Although considerably simplified, the reduced order model presented in this paper provides valuable insight about the control strategy for bilateral feedback on dynamic balancing teleoperation. For instance, increasing sensitivity

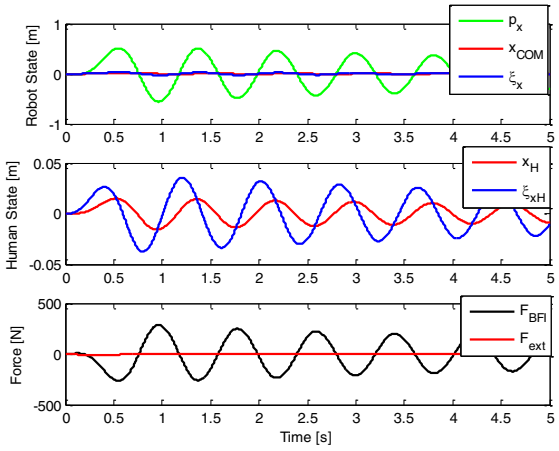

Fig. 9. Simulated marginally stable coupled system dynamics for large mapping gain $\alpha = 3\ rad/s$.

of the mapping gain α is one of the major causes of ringing (marginal stability) or even instability for the bilateral feedback teleoperation. At the same time, due to the nature of the lightly damped human CoM dynamics, high gains for the BFI force can also compromise the system performance.

In section III, we provide some insight about the advantages of the negative feedback convention adopted for the presented experiments. Further work that explores the opposing ideas of negative or positive feedback to the human can provide a definitive answer on the best performance controller for reflex-based reactions.

The ultimate goal of this project is to allow robots to achieve highly dynamic manipulation capabilities for large momentum delivery tasks. Such tasks require instantaneous loss of balancing control authority in order to build momentum and are followed by a reaction motion to recapture stability. These behaviors can be observed, for instance, when firefighters use body momentum to enhance the effective hit of an ax while breaking trough a wall. We hypothesize that we can transfer this same intelligence to the robot using mutual learning strategies during bilateral feedback teleoperation.

The framework proposed in this paper presents a glimpse on how to intuitively take advantage of human natural motor skills during whole-body teleoperation. Future work intends to include angular and linear momentum regulation on the balancing controller [20], similar to human reaction strategies.

VI. Acknowledgments

This work is funded by the DARPA Young Faculty Award.

References

[1] Pratt, Carff, Drakunov, and Goswami, "Capture point: A step toward humanoid push recovery," in *Humanoid Robots, 2006 6th IEEE-RAS International Conference on*. IEEE, 2006.

[2] Koolen, Boer, Rebula, and Goswami, "Capturability-based analysis and control of legged locomotion, part 1: Theory and application to three simple gait models," *Robotics Research, International Journal on*, 2012.

[3] N. Hogan, "Adaptive control of mechanical impedance by coactivation of antagonist muscles," *Automatic Control, IEEE Transactions on*, vol. AC-29, no. 8, 1984.

[4] Wang, Ramos, Mayo, Ubellacker, and Kim, "The hermes humanoid system: A platform for full-body teleoperation with balance feedback," in *Humanoid Robots, 2015 15th IEEE-RAS International Conference on*. IEEE, 2015.

[5] Ramos, Wang, Mayo, Ubellacker, and Kim, "A balance feedback interface for whole-body teleoperation of a humanoid robot and implementation in the hermes system," in *Humanoid Robots, 2015 15th IEEE-RAS International Conference on*. IEEE, 2015.

[6] Takenaka, Matsumoto, and Yoshiike, "Real time motion generation and control for biped robot -1st report: Walking gait pattern generation," in *Intelligent Robots and Systems (IROS), 2009 IEEE/RSJ International Conference on*. IEEE, 2009.

[7] Hopkins, Hong, and Leonessa, "Humanoid locomotion on uneven terrain using the time-varying divergent components of motion," in *Humanoid Robots, 2014 14th IEEE-RAS International Conference on*. IEEE, 2014.

[8] Englsberger, Ott, and Albu-Schaffer, "Three-dimensional bipedal walking control using divergent component of motion," in *Intelligent Robots and Systems (IROS), 2013 IEEE/RSJ International Conference on*. IEEE, 2013.

[9] L. Hof, "The extrapolated center of mass concept suggests a simple control of balancing in walking," *Human Motion Science*, vol. 27, no. 1, pp. 112–125, 2008.

[10] Hopkins, Hong, and Leonessa, "Compliant Locomotion Using Whole-Body Control and Divergent Component of Motion Tracking," in *Robotics and Automation (ICRA), 2015 IEEE International Conference on*. IEEE, 2015.

[11] Morisawa, Kajita, Kanehiro, Kaneko, Miura, and Yokoi, "Balance control based on capture point error compensation for biped walking on uneven terrain," in *Humanoid Robots, 2012 12th IEEE-RAS International Conference on*. IEEE, 2012.

[12] J. Koenemann, "Real-time Imitation of Human Whole-Body Motions by Humanoids," in *Robotics and Automation (ICRA), 2014 IEEE International Conference on*. IEEE, 2014.

[13] S. Kim, C. Kim, B. You, and S. Oh, "Stable whole-body motion generation for humanoid robots to imitate human motions," in *Intelligent Robots and Systems (IROS), 2009 IEEE/RSJ International Conference on*. IEEE, 2009.

[14] T. Takubo, K. Inoue, and T. Arai, "Whole-body teleoperation for humanoid robot by marionette system," in *Intelligent Robots and Systems (IROS), 2006 IEEE/RSJ International Conference on*. IEEE, 2006.

[15] Neo, Yokoi, Kajita, and Tanie, "Whole-body motion generation integrating operators intention and robots autonomy in controlling humanoid robots," *IEEE Transactions on Robotics*, vol. 23, no. 4, 2007.

[16] L. Peternel and J. Babic, "Humanoid Robot Posture-Control Learning in Real-Time Based on Human Sensorimotor Learning Ability," in *Robotics and Automation (ICRA), 2013 IEEE International Conference on*. IEEE, 2013.

[17] Peternel and Babic, "Learning of compliant humanrobot interaction using full-body haptic interface," *Advanced Robotics*, vol. 27, 2013.

[18] R. Vuga, M. Ogrinc, A. Gams, T. Petric, N. Sugimoto, A. Ude, and J. Morimoto, "Motion Capture and Reinforcement Learning of Dynamically Stable Humanoid Movements Primitives," in *Robotics and Automation (ICRA), 2013 IEEE International Conference on*. IEEE, 2013.

[19] E. Burdet, D. Franklin, and T. Milner, *Human Robotics: Neuromechanics and Motor Control*. The MIT Press, 2013, vol. 5.

[20] Orin, Goswami, and Lee, "Centroidal dynamics of a humanoid robot," *Journal on Autonomous Robots*, vol. 35, pp. 161–167, 2013.

[21] T. Sugihara, "Standing Stabilizability and Stepping Maneuver in Planar Bipedalism based on the Best COM-ZMP Regulator," in *Robotics and Automation (ICRA), 2009 IEEE International Conference on*. IEEE, 2009.